Physica D 421 (2021) 132859

Contents lists available at ScienceDirect

Physica D

journal homepage: www.elsevier.com/locate/physd

Mathematical formulation of a dynamical system with dry friction subjected to external forces

A. Bensoussan [a,b,1], A. Brouste [c,1], F.B. Cartiaux [d,1], C. Mathey [e,1], L. Mertz [f,1,*]

[a] Jindal School of Management, University of Texas at Dallas, Richardson, USA
[b] School of Data Science, Hong-Kong City University, Hong Kong
[c] Laboratoire Manceau de Mathématiques, Le Mans Université, Le Mans, France
[d] OSMOS Group, France
[e] Department of Mathematics, City University of Hong Kong, Kowloon Tong, Hong Kong
[f] ECNU-NYU, Institute of Mathematical Sciences, NYU Shanghai, Shanghai, China

ARTICLE INFO

Article history:
Received 28 January 2020
Received in revised form 25 January 2021
Accepted 27 January 2021
Available online 6 February 2021
Communicated by T. Insperger

Keywords:
Dry friction
Extended variational inequality
Model calibration

ABSTRACT

We consider the response of a one-dimensional system with friction. Shaw (1986) introduced the set up of different coefficients for the static and dynamic phases (also called stick and slip phases). He constructs a step by step solution, corresponding to an harmonic forcing. In this paper, we show that the theory of variational inequalities (V.I.) provides an elegant and synthetic approach to obtain the existence and uniqueness of the solution, avoiding the step by step construction. We then apply the theory to a real structure with real data and show that the model qualitatively agrees with the real data. In our case, the forcing motion comes from dilatation, due to temperature.

1. Introduction

The study of one dimensional models of *dry friction* (also called *Coulomb friction*) has received a significant interest over the last decades [1–6]. A typical example is a solid lying on a motionless surface. In response to forces, the dynamics of the solid has two separate phases. One is *dynamic* (also called slip) in which the solid moves and a dynamic friction force opposes the motion. The other phase is *static* (also called stick) in which the solid remains motionless while being subjected to a static friction force that is necessary for equilibrium. The physics of dry friction is presented in [7,8]. The static phase plays an important role on the prediction of the system behavior (e.g. failure) and thus it has to be carefully analyzed.

The case when external forces are harmonic has been investigated with particular attention. Two classes of techniques have been developed in the literature. In dimension one or two, *exact methods* have been considered. Den Hartog [1] has proposed an exact solution of the dynamic phase for a single degree of freedom system where the coefficients of static and dynamic friction are equal. Shaw [2] extended Den Hartog's results with a different approach to the case where the coefficients of static and dynamic friction are not identical and provided a stability analysis of the periodic motion. Yeh [4] extended the method to two degrees of freedom with one dry friction damper. In higher dimensions, an approximation method called *the incremental harmonic balance (IHB) method*, has been developed by Lau, Cheung & Wu [5,6] and Pierre, Ferri & Dowel [3]. This method is efficient when dealing with many degrees of freedom and many dry friction dampers. The IHB method does provide good results on amplitude and phase for a broad class of stick/slip motions but it does not give detailed information about stick/slip phases.

In this paper, we study a one-dimensional problem, with general forcing term. Denoting the actual displacement of the oscillator by x, we consider the initial value problem

$$m\ddot{x}(t) + \mathbb{F}(\dot{x}(t)) = b(x(t), t), \ t > 0 \tag{1}$$

with $m > 0$ is a constant, the initial displacement and velocity

$$x(0) = x_0, \quad \dot{x}(0) = 0. \tag{2}$$

On the right hand side of Eq. (1), $b(x(t), t)$ represents the forces that are not related to dry friction; here b is a locally Lipschitz function with at most linear growth. The considered system is a one degree of freedom oscillator. Thus, although variable x is one-dimensional, the phase-space of the dynamical system is two-dimensional. In our application, we will take

$$b(x, t) \triangleq K(\beta T(t) - x) \tag{3}$$

with K, β constants and T is a temporal function which describes the evolution of the temperature. The function $\mathbb{F}(\dot{x}(t))$ is not easy

* Corresponding author.
E-mail address: laurent.mertz@nyu.edu (L. Mertz).

[1] The authors declare that they have contributed equally to the work reported in this paper.

https://doi.org/10.1016/j.physd.2021.132859
0167-2789/

to describe. In a static phase $\dot{x}(t) = 0$ on an interval, which implies $\ddot{x}(t) = 0$ on the same interval and therefore from (1)

$$\mathbb{F}(\dot{x}(t)) = b(x(t), t). \tag{4}$$

However, this is possible only when $|b(x(t), t)| \leq f_s$, where f_s is the static friction coefficient.[2] In a dynamic phase $\dot{x}(t) \neq 0$ on an interval, although it can vanish at isolated points. We cannot simply use Eq. (1) to obtain $\mathbb{F}(\dot{x}(t))$. We need an additional information, provided by Coulomb's law. We write, formally

$$\mathbb{F}(\dot{x}(t)) = f_d \text{sign}(\dot{x}(t)). \tag{5}$$

Since we expect $\dot{x}(t)$ to vanish only at isolated points, $\text{sign}(\dot{x}(t))$ is defined almost everywhere, and therefore, we can use this expression in the second order differential equation (1), with an equality valid a.e. instead of for any t. The difficulty is that we cannot write the equation a priori. The step by step construction of the solution is a way to get out of this dilemma. A more elegant way is to use variational inequalities (V.I.) [9]. A V.I. is the following mathematical problem: find a continuously differentiable function $x(.)$ that satisfies

$$\forall t > 0, \forall \varphi \in \mathbb{R}, (b(x(t), t) - m\ddot{x}(t))(\varphi - \dot{x}(t)) + f_d|\dot{x}(t)| \leq f_d|\varphi|. \quad (\mathcal{VI})$$

If we apply the V.I. in a static phase, when $\dot{x}(t) = 0$ on an interval, we get immediately that $|b(x(t), t)| \leq f_d$. This cannot apply to the case considered by Shaw in which in a static phase $|b(x(t), t)| \leq f_s$ with a coefficient $f_s > f_d$. We will see how to solve this difficulty in the next section.

Remark 1. We can change $b(x(t), t)$ into $b(x(t), \dot{x}(t), t)$ on the right hand side of Eq. (1), provided the dependence in $\dot{x}(t)$ is smooth. For instance, we have in mind forces of the form $b(x(t), \dot{x}(t), t) = b(x(t), t) - \alpha\dot{x}(t)$. To simplify we shall omit this situation.

Remark 2. Our approach lies in the framework of Den Hartog [1] and Shaw [2]. We want to emphasize the interest of V.I. in providing a synthetic and rigorous mathematical analysis of the problem. It is of course known that V.I. are an important tool for nonlinear problems of mechanics, like elastic–plastic systems and contact friction models based on Signorini's Law and Coulomb's Law, see Lebon [10] and references therein. Another mathematical theory, which is widely used, is the theory of differential inclusions; see Manuel Marques [11], Bastien and Schatzman [12]. This theory is more general than that of V.I. but presents the difficulty of obtaining non unique solutions. Since the systems, which are considered are nonlinear dynamical systems, one finds in the literature many works related to the behavior of non-smooth dynamical systems, see di Bernado, Budd, [13] including the possibility of chaotic behavior, see Licsko [14], and that of "shake down", see Klarbling [15]. These aspects of non-smooth dynamical systems are not directly related to our work. We prefer V.I. to differential inclusions, because we can obtain uniqueness. The closest work related to ours on numerical simulation is [16]. The work of Lebon is directly on V.I. but in a more complex set up, in dimension 2, with both Signorini and Coulomb law acting. This leads to a system of coupled V.I., for which the author studies specific algorithms. In our work we remain in the one-dimensional classical set up of Den Hartog, Shaw with the sequence of static-dynamic phases. We make an extensive comparison of the use of V.I. and of the step-by-step construction of the trajectory, which in fact requires splitting the dynamic phase into sub phases.

In this paper, we propose a two-phase model for Eqs. (1)–(2) with $f_d \leq f_s$ and obtain a solution which is C^1. The two phases are called static and dynamic phases. The dynamic phase is captured by a V.I. In the case $f_d = f_s$, the VI captures both phases.

[2] Since f_s has to be compared with the magnitude of $|b(x(t), t)|$, it has the same dimension as $|b(x(t), t)|$ and thus can be seen as a force like-term.

2. Model description and mathematical theory

2.1. Description of dry friction: static and dynamic phases

In presence of dry friction, the physical description of the dynamic and static phases is as follows.

- The phase of $x(t)$ at time t is **static** when

  $\dot{x}(t) = 0$ and $|b(x(t), t)| \leq f_s$.

  It is important to emphasize that a static phase corresponds to $\dot{x}(t) = 0$ on a time interval of positive Lebesgue measure and thus $\ddot{x}(t) = 0$ on the same interval. In this case, the friction force takes the value

  $\mathbb{F}(\dot{x}(t)) = b(x(t), t)$

  that is necessary for equilibrium.
- Otherwise, the phase of $x(t)$ at time t is **dynamic** when

  $\dot{x}(t) = 0$ and $|b(x(t), t)| > f_s$ or $\dot{x}(t) \neq 0$.

  When $\dot{x}(t) \neq 0$, the friction force takes the value

  $\mathbb{F}(\dot{x}(t)) = \text{sign}(\dot{x}(t))f_d$.

  It is important to emphasize that $\dot{x}(t) = 0$ and $|b(x(t), t)| > f_s$ happen on a negligible (isolated points) time set.

The transition from a static phase to a dynamic phase occurs as soon as

$$|b(x(t), t)| > f_s.$$

Conversely, from a dynamic phase the system enters into a static phase as soon as

$$\dot{x}(t) = 0 \text{ and } |b(x(t), t)| \leq f_s.$$

Below, we make precise the mathematical formulation and obtain a solution which is C^1.

2.2. Mathematical theory: an extended variational inequality (E.V.I.) formulation for the two phase model

We first assume that $f_s > f_d$. We will discuss the case $f_s = f_d$ at the end of this section in Remark 4. We want to define rigorously a function $x(t)$, which is C^1 and satisfies the set of conditions (static/dynamic phase, transition from dynamic to static phase and vice versa.) (1), (2), (3), (4) and (5). We define it, as follows: we look for a function $x \in C^1(\mathbb{R}^+)$. We associate to this function the domain in $\mathbb{R}^+$ defined by

$$\mathcal{O}_{x(.)} \triangleq \{t > 0,\ |b(x(t), t)| > f_s\} \cup \{t > 0,\ |\dot{x}(t)| > 0\}. \tag{6}$$

This is an open domain in $\mathbb{R}^+$. In this domain $x(t)$ is the solution of the variational inequality

$$\forall \varphi \in \mathbb{R},\ \forall \text{ a.e. } t \in \mathcal{O}_{x(.)},\ (b(x(t), t) - m\ddot{x}(t))(\varphi - \dot{x}(t)) + f_d|\dot{x}(t)| \leq f_d|\varphi|. \tag{7}$$

We need to add initial conditions $x(0)$ and $\dot{x}(0)$. We assume that the system starts from a static phase,

$$|b(x(0), 0)| \leq f_s \text{ and } \dot{x}(0) = 0. \tag{8}$$

We claim that the conditions (6), (7) and the initial condition (8) define a unique function $x(t) \in C^1(\mathbb{R}^+)$. Note that the complement of $\mathcal{O}_{x(.)}$ is the closed subset of $\mathbb{R}^+$

$$\mathcal{CO}_{x(.)} \triangleq \{t \geq 0,\ |b(x(t), t)| \leq f_s\} \cap \{t \geq 0,\ \dot{x}(t) = 0\} \tag{9}$$

and the boundary of $\mathcal{O}_{x(.)}$ is

$$\partial\mathcal{O}_{x(.)} \triangleq \{t \geq 0,\ |b(x(t), t)| = f_s\} \cap \{t \geq 0,\ \dot{x}(t) = 0\}. \tag{10}$$

We first state the first lemma.

Lemma 1. *In $\mathcal{O}_{x(.)}$, we have $\dot{x} \neq 0$ a.e.*

Proof. Let $t_0 \in \mathcal{O}_{x(.)}$ such that $\dot{x}(t_0) = 0$, we cannot find $\epsilon > 0$ such that $[t_0, t_0 + \epsilon) \subset \mathcal{O}_{x(.)}$ and $\forall t \in [t_0, t_0 + \epsilon)$, $\dot{x}(t) = 0$. Indeed, if such ϵ exists, then $\forall t \in [t_0, t_0 + \epsilon)$, $|b(x(t), t)| > f_s$. Moreover $\forall t \in (t_0, t_0 + \epsilon)$, $\ddot{x}(t) = 0$ and from the V.I. (7) it follows $\forall \varphi \in \mathbb{R}$, $\forall t \in (t_0, t_0 + \epsilon)$, $b(x(t), t)\varphi \leq f_d|\varphi|$ which implies $\forall t \in (t_0, t_0 + \epsilon)$, $|b(x(t), t)| \leq f_s$. Thus we obtain a contradiction. Similarly, we cannot have $(t_0 - \epsilon, t_0] \subset \mathcal{O}_{x(.)}$ and $\forall t \in (t_0 - \epsilon, t_0]$, $\dot{x}(t) = 0$. So t_0 is an isolated point in $\mathcal{O}_{x(.)}$, which implies the result. □

It follows that sign $(\dot{x}(t))$ is defined a.e. Therefore, we can replace the V.I. (7), by

$$\forall \text{a.e. } t \in \mathcal{O}_{x(.)},\ m\ddot{x}(t) = b(x(t), t) - f_d \text{sign}\dot{x}(t). \tag{11}$$

In this context, the open set $\mathcal{O}_{x(.)}$ is called the dynamic phase of the trajectory $x(t)$. Its complement is the static phase. The existence and uniqueness of a solution of the E.V.I. formulation (6), (7) and (8) are shown in the theorem below.

Theorem 1. *Assume $f_s > f_d$. Then, there exists one and only one solution of (6), (7) and (8).*

Proof. We first prove the existence. We are going to define a sequence $\{\tau_j, x_j\}_{j\geq 0}$. We begin with $\tau_0 = 0$ and $x_0 = x(0)$ the initial condition. From (8), $|b(x_0, \tau_0)| \leq f_s$ and $\dot{x}(\tau_0) = 0$. More generally, suppose we have a pair τ_j, x_j with $|b(x_j, \tau_j)| \leq f_s$ and $\dot{x}(\tau_j) = 0$. We then define $\tau_{j+\frac{1}{2}} \triangleq \inf\{t > \tau_j,\ |b(x(t), t)| > f_s\}$. We may have $\tau_j = \tau_{j+\frac{1}{2}}$. If $\tau_{j+\frac{1}{2}} > \tau_j$ then we define $\forall t \in [\tau_j, \tau_{j+\frac{1}{2}}]$, $x(t) = x_j$ and $\dot{x}(t) = 0$. We consider next the variational inequality

$$\forall \varphi \in \mathbb{R}, \forall \text{a.e.} t > \tau_{j+\frac{1}{2}}, (b(x(t), t) - m\ddot{x}(t))(\varphi - \dot{x}(t)) + f_d|\dot{x}(t)| \leq f_d|\varphi| \tag{12}$$

with $x(\tau_{j+\frac{1}{2}}) = x_j$ and $\dot{x}(\tau_{j+\frac{1}{2}}) = 0$. This class of V.I. is standard and the theory tells that such a problem has one and one solution in C^1 on the interval $(\tau_{\frac{1}{2}}, \infty)$. We shall not give a proof of this general result but discuss the properties of the solution in the next section. We then define τ_{j+1} by the condition

$$\tau_{j+1} \triangleq \inf\{t > \tau_{j+\frac{1}{2}},\ \dot{x}(t) = 0 \quad \text{and} \quad |b(x(t), t)| \leq f_s\}.$$

We have $\tau_{j+1} > \tau_{j+\frac{1}{2}}$. It is justified in 4 steps.

Step 1.

Using the continuity of the function $t \mapsto b(x(t), t)$ and the fact that $|b(x_j, \tau_{j+\frac{1}{2}})| = f_s$, there exists a $\delta > 0$ such that

$$\forall t \in (\tau_{j+\frac{1}{2}}, \tau_{j+\frac{1}{2}} + \delta),\ |b(x(t), t)| \geq \frac{f_s + f_d}{2} > f_d. \tag{13}$$

Step 2.

It is not possible to find a subinterval $I \subset (\tau_{j+\frac{1}{2}}, \tau_{j+\frac{1}{2}} + \delta)$ of positive Lebesgue measure such that $\dot{x}(t) = 0$. For the sake of contradiction, suppose there exists such an interval I where $\forall t \in I$, $\dot{x}(t) = 0$. Then we must have $\forall t \in I$, $\ddot{x}(t) = 0$ and as a consequence of the V.I. (12), we have $\forall t \in I$, $|b(x(t), t)| \leq f_d$. This is a contradiction with (13).

As a consequence, zeros of $\dot{x}$ (if any) are isolated points on the interval $(\tau_{j+\frac{1}{2}}, \tau_{j+\frac{1}{2}} + \delta)$. This implies that the function $t \mapsto \text{sign}(\dot{x}(t))$ is defined a.e. on $(\tau_{j+\frac{1}{2}}, \tau_{j+\frac{1}{2}} + \delta)$.

Step 3.

So, outside of a set of measure 0, $\dot{x}$ is either positive or negative. Therefore, on the interval $(\tau_{j+\frac{1}{2}}, \tau_{j+\frac{1}{2}} + \delta)$, the V.I. (12) is equivalent to $m\ddot{x}(t) = b(x(t), t) - f_d \text{sign}(\dot{x}(t))$.

Step 4.

Thus from (13), if $b(x(t), t) \geq \frac{f_s + f_d}{2}$ on $(\tau_{j+\frac{1}{2}}, \tau_{j+\frac{1}{2}} + \delta)$ then on the same interval $\ddot{x}(t) \geq \frac{f_s - f_d}{2m} > 0$. In turn, it gives $\dot{x}(\tau_{j+\frac{1}{2}} + h) \geq h\frac{f_s - f_d}{2m}$ for any h small enough and $\forall t \in (\tau_{j+\frac{1}{2}}, \tau_{j+\frac{1}{2}} + \delta)$, $\dot{x}(t) > 0$. In this case, $\text{sign}(\dot{x}(t)) = 1$.

Similarly, if $b(x(t), t) \leq -\frac{f_s + f_d}{2}$ on $(\tau_{j+\frac{1}{2}}, \tau_{j+\frac{1}{2}} + \delta)$ then on the same interval $\ddot{x}(t) \leq -\frac{f_s - f_d}{2m} < 0$. $\dot{x}(\tau_{j+\frac{1}{2}} + h) \leq -h\frac{f_s - f_d}{2m}$ provided that h is small enough and $\forall t \in (\tau_{j+\frac{1}{2}}, \tau_{j+\frac{1}{2}} + \delta)$, $\dot{x}(t) < 0$. In this case, $\text{sign}(\dot{x}(t)) = -1$. All in all, this proves $\tau_{j+1} > \tau_{j+\frac{1}{2}}$. Furthermore, next we check that the zeros of $\dot{x}$, if any, are isolated on the interval $(\tau_{j+\frac{1}{2}}, \tau_{j+1})$. Consider $t^\star$ in this interval such that $x(t^\star) = 0$. Since $t^\star < \tau_{j+1}$, necessarily $|b(x(t^\star), t^\star))| > f_s$. But then, as in Lemma 1, there cannot be a small interval around $t^\star$ on which $\dot{x}(t)$ vanishes. This implies that the function $t \mapsto \text{sign}(\dot{x}(t))$ is defined a.e. on $(\tau_{j+\frac{1}{2}}, \tau_{j+1})$. We therefore can replace the VI by $\forall \text{a.e.} t \in (\tau_{j+\frac{1}{2}}, \tau_{j+1})$

$$\begin{cases} m\ddot{x}(t) + f_d \text{sign}(\dot{x}(t)) = b(x(t), t), \\ x(\tau_{j+\frac{1}{2}}) = x_j, \quad \dot{x}(\tau_{j+\frac{1}{2}}) = 0. \end{cases} \tag{14}$$

It is possible to have $\tau_{j+1} = \infty$. If $\tau_{j+1} < \infty$ we can set $x_{j+1} \triangleq x(\tau_{j+1})$. In this way, we have defined the value x_{j+1}, τ_{j+1} starting from x_j, τ_j. We have $\tau_{j+1} > \tau_j$ and also the sequence $\tau_j \to \infty$ as $j \to \infty$. For the sake of contradiction, suppose $\tau_j \to \theta < \infty$ and so does the sequence $\tau_{j+\frac{1}{2}}$. From Eq. (14), with $t = \tau_{j+\frac{1}{2}}$, we must have

$$m\ddot{x}(\tau_{j+\frac{1}{2}} + 0) + f_d \text{sign}(\dot{x}(\tau_{j+\frac{1}{2}} + 0)) = b(x(\tau_{j+\frac{1}{2}}), \tau_{j+\frac{1}{2}}),$$

and thus

$$m|\ddot{x}(\tau_{j+\frac{1}{2}} + 0)| = f_s - f_d > 0.$$

But $\ddot{x}(\tau_{j+1} + 0) = 0$. So the sequence τ_j cannot converge toward a finite value as it would lead to a contradiction. We have defined a function $x(t)$ which is C^1 and satisfies (6)–(7)–(8). It is the only one. Indeed, if $x(t)$ is a solution of (6)–(7)–(8), then we define $\tau_{\frac{1}{2}}$, in which the trajectory $x(t)$ enters in $\mathcal{O}_{x(.)}$. The V.I. holds. This allows us to define τ_1, the time at which the trajectory leaves $\mathcal{O}_{x(.)}$ to enter the static phase. Continuing we obtain the sequence of times τ_j defined for the existence. So the trajectory $x(t)$ coincides with that constructed for the existence. This completes the proof. □

Remark 3. In the proof of Theorem 1, we would like to emphasize that the V.I. of type (14) on $(\tau_{j+\frac{1}{2}}, \tau_{j+1})$ is equivalent to (14) together with the fact that the zeros of $\dot{x}(t)$ are isolated points. But one needs to define τ_{j+1} which depends on the equation. We cannot just write Eq. (14) after $\tau_{j+\frac{1}{2}}$ because we cannot define the function $\text{sign}(\dot{x}(t))$ without prior knowledge that the zeros of $\dot{x}(t)$ are isolated. We need to define a well posed problem, valid for any time posterior to $\tau_{j+\frac{1}{2}}$. Eq. (14) cannot be used. The V.I. is an elegant way to fix this difficulty. The only alternative is to construct the trajectory in the dynamic phase step by step, as we are going to do in the next section. The V.I. is a synthetic way to define the solution, without a lengthy construction. As we shall see, when $f_s = f_d$, it will also incorporate the static phase, and thus avoid any sequence of intervals.

Remark 4. The mathematical formulation of the E.V.I. above is equivalent to a V.I. when $f \triangleq f_s = f_d$. Indeed, assume $y(.)$ is a C^1 function and satisfies

$$\forall \varphi \in \mathbb{R},\ \forall \text{a.e. } t \geq 0,\ (b(y(t),t) - m\ddot{y}(t))(\varphi - \dot{y}(t)) + f|\dot{y}(t)| \leq f|\varphi| \tag{15}$$

where the initial conditions are the same as in (8) $y(0) = x(0)$ and $\dot{y}(0) = 0$ ($|b(y(0),0)| \leq f$ and $\dot{y}(0) = 0$). To this function, we can define the open domain $\mathcal{O}_{y(.)} \triangleq \{t > 0,\ |b(y(t),t)| > f\} \cup \{t > 0,\ |\dot{y}(t)| > 0\}$ in which the V.I. is satisfied. Thus, $y(.)$ satisfies the notion of E.V.I. in (6)–(7)–(8). We now check the reverse. Suppose $x(.)$ is C^1 and satisfies (6)–(7)–(8). We claim that the V.I. is also satisfied on $\text{Int}(\mathcal{CO}_{x(.)})$, the interior of $\mathcal{CO}_{x(.)}$. If $\text{Int}(\mathcal{CO}_{x(.)})$ is empty then the V.I. holds almost everywhere. Otherwise, $\text{Int}(\mathcal{CO}_{x(.)})$ is an open set of positive measure on which we have $|b(x(t),t)| \leq f$, $\dot{x}(t) = 0$ and $\ddot{x}(t) = 0$. This means that the V.I. is also satisfied on $\text{Int}(\mathcal{CO}_{x(.)})$ and then almost everywhere. Thus $x(.)$ is a C^1 function satisfying (15).

2.3. A step by step method for the dynamic phase as an alternative to the V. I

2.3.1. A general formulation for the sub phases of the dynamic phase

We now check that we can also define a sequence of sub phases of the dynamic phase, in which the solution satisfies a standard differential equation. This procedure is an alternative to the V.I. but is much less synthetic. The first dynamic sub-phase starts at $\tau_{\frac{1}{2}} \triangleq \inf\{t > \tau_0,\ |b(x(t),t)| > f_s\}$ where we recall that $\tau_0 \triangleq 0$. Define

$$x_0^0 \triangleq x(0), \quad \tau_0^0 \triangleq \tau_{\frac{1}{2}},$$

thus

$$|b(x_0^0, \tau_0^0)| = f_s.$$

We set $\epsilon_0^0 \triangleq \text{sign}(b(x_0^0, \tau_0^0))$ and consider the differential equation

$$\begin{cases} m\ddot{x}(t) = b(x(t),t) - \epsilon_0^0 f_d,\ t > \tau_0^0, \\ x(\tau_0^0) = x_0^0, \quad \dot{x}(\tau_0^0) = 0. \end{cases} \tag{16}$$

Then, we define

$$\tau_0^1 \triangleq \inf\{t > \tau_0^0,\ \dot{x}(t) = 0\} \quad \text{and} \quad x_0^1 \triangleq x(\tau_0^1).$$

- If $|b(x_0^1, \tau_0^1)| \leq f_s$ then the dynamic phase ends here and a new static phase starts. We set

  $$\tau_1 \triangleq \tau_0^1 \quad \text{and} \quad x_1 \triangleq x_0^1.$$

- Otherwise $|b(x_0^1, \tau_0^1)| > f_s$ and we set

  $$\epsilon_0^1 \triangleq \text{sign}(b(x_0^1, \tau_0^1))$$

  and again consider the differential equation

  $$\begin{cases} m\ddot{x}(t) = b(x(t),t) - \epsilon_0^1 f_d,\ t > \tau_0^1, \\ x(\tau_0^1) = x_0^1, \quad \dot{x}(\tau_0^1) = 0 \end{cases} \tag{17}$$

  and introduce

  $$\tau_0^2 \triangleq \inf\{t > \tau_0^1,\ \dot{x}(t) = 0\}.$$

  We can repeat the same procedure several times and thus define a sequence $\tau_0^k, x_0^k, \epsilon_0^k$ for $k \leq k(0)$ where

  $$k(0) \triangleq \inf\{k \geq 1,\ |b(x_0^k, \tau_0^k)| \leq f_s\}.$$

  If $k(0) = \infty$ then x remains in a dynamic phase forever otherwise a new static phase starts at

  $$\tau_1 \triangleq \tau_0^{k(0)} \quad \text{and} \quad x_1 \triangleq x_0^{k(0)}.$$

  The dynamic phase on the interval $(\tau_{\frac{1}{2}}, \tau_1)$ is thus divided into dynamic sub-phases (τ_0^k, τ_0^{k+1}) with

  $$\tau_0 \leq \tau_{\frac{1}{2}} = \tau_0^0 < \tau_0^1 < \cdots < \tau_0^{k(0)} = \tau_1.$$

Similarly, if for any $j \geq 1$ we know x_j and τ_j with $|b(x_j, \tau_j)| \leq f_s$. The first dynamic sub phase starts at

$$\tau_j^0 \triangleq \tau_{j+\frac{1}{2}},\ x_j^0 \triangleq x_j,\ \text{where } |b(x_j^0, \tau_j^0)| = f_s.$$

For each $k \geq 0$, to define the dynamic sub phase starting at τ_j^k, we set

$$\epsilon_j^k \triangleq \text{sign}(b(x_j^k, \tau_j^k))$$

and consider the differential equation

$$\begin{cases} m\ddot{x}(t) = b(x(t),t) - \epsilon_j^k f_d,\ t > \tau_j^k, \\ x(\tau_j^k) = x_j^k, \quad \dot{x}(\tau_j^k) = 0. \end{cases} \tag{18}$$

Then, we uniquely define τ_j^{k+1} by

$$\tau_j^{k+1} \triangleq \inf\{t > \tau_j^k, \dot{x}(t) = 0\}.$$

This procedure defines the dynamic sub phase (τ_j^k, τ_j^{k+1}). On this subinterval $\epsilon_j^k = \text{sign}(\dot{x}(t))$, so (18) is also the equation

$$m\ddot{x}(t) = b(x(t),t) - \text{sign}(\dot{x}(t)) f_d. \tag{19}$$

We set $x_j^{k+1} \triangleq x(\tau_j^{k+1})$ and we proceed as follows:

- if $|b(x_j^{k+1}, \tau_j^{k+1})| \leq f_s$ then we start a new static phase and we set

  $$\tau_{j+1} \triangleq \tau_j^{k+1} \text{ and } x_{j+1} \triangleq x_j^{k+1}.$$

- on the other hand, if $|b(x_j^{k+1}, \tau_j^{k+1})| > f_s$ then we start a new dynamic sub phase on the interval $(\tau_j^{k+1}, \tau_j^{k+2})$.

We can define

$$k(j) \triangleq \inf\{k \geq 1,\ |b(x_j^k, \tau_j^k)| \leq f_s\},$$

thus the dynamic phase on the interval $(\tau_{j+\frac{1}{2}}, \tau_{j+1})$ is divided into dynamic sub-phases (τ_j^k, τ_j^{k+1}) with

$$\tau_j \leq \tau_{j+\frac{1}{2}} = \tau_j^0 < \tau_j^1 < \cdots < \tau_j^{k(j)} = \tau_{j+1}.$$

This procedure gives explicitly the solution of the V.I. We will see in the next section that, when considering the case $b(x,t) = K(\beta T(t) - x)$, we have the additional advantage that the solution is explicit in a dynamic sub phase.

2.3.2. Formula for $x(t)$ on a dynamic sub phase when $b(x,t) = K(\beta T(t) - x)$

When $b(x,t) = K(\beta T(t) - x)$, the differential equation (18) has an explicit solution. For $t \in [\tau_j^k, \tau_j^{k+1})$,

$$x(t) = x_j^k \cos\omega\left(t - \tau_j^k\right) + \int_{\tau_j^k}^t \sin\omega(t-s)\frac{K\beta T(s) - \epsilon_j^k f_d}{m\omega}\text{d}s \tag{20}$$

and τ_j^{k+1} is defined by the equation

$$x_j^k \sin\omega\left(\tau_j^{k+1} - \tau_j^k\right) = \int_{\tau_j^k}^{\tau_j^{k+1}} \cos\omega(\tau_j^{k+1} - s)\frac{K\beta T(s) - \epsilon_j^k f_d}{m\omega}\text{d}s. \tag{21}$$

We then set

$$x_j^{k+1} \triangleq x(\tau_j^{k+1}) = x_j^k \cos\omega\left(\tau_j^{k+1} - \tau_j^k\right) + \int_{\tau_j^k}^{\tau_j^{k+1}} \sin\omega(\tau_j^{k+1} - s) \times \frac{K\beta T(s) - \epsilon_j^k f_d}{m\omega} \mathrm{d}s. \tag{22}$$

2.3.3. Construction of the sequence $\{x_j, \tau_j\}$ and the trajectory $\{x(t), t \geq 0\}$ when $b(x,t) = K(\beta T(t) - x)$

The above discussion allows to define an algorithm to construct the trajectory $x(t)$ of initial problems (1) and (2) with $b(x,t)$ given in (3). We construct the sequence $\{x_j, \tau_j, j \geq 0\}$ where

$$|b(x_j, \tau_j)| \leq f_s.$$

When $j = 0$, it corresponds to the initial condition $x_0 \triangleq x(0)$ and $\tau_0 \triangleq 0$. For each $j \geq 0$, we first compute

$$\tau_{j+\frac{1}{2}} \triangleq \inf\{t \geq \tau_j,\ |b(x_j, t)| > f_s\}$$

and then we define a subsequence with respect to k.

- Define

  $$\tau_j^0 \triangleq \tau_{j+\frac{1}{2}}, \quad x_j^0 \triangleq x_j, \quad \epsilon_j^0 \triangleq \mathrm{sign}(b(x_j^0, \tau_j^0)).$$

- For each $k \geq 0$, using ϵ_j^k, define τ_j^{k+1} using (21) and x_j^{k+1} using (22).
- If

  $$|b(x_j^{k+1}, \tau_j^{k+1})| \leq f_s$$

  then

  $$\tau_{j+1} \triangleq \tau_j^k \text{ and } x_{j+1} \triangleq x_j^{k+1}$$

  otherwise we define

  $$\epsilon_j^{k+1} \triangleq \mathrm{sign}(b(x_j^{k+1}, \tau_j^{k+1}))$$

  and repeat the procedure with the definition of τ_j^{k+2}, x_j^{k+2}.

The subinterval $(\tau_j, \tau_{j+\frac{1}{2}})$ is a static or stick subphase, and the subinterval $(\tau_{j+\frac{1}{2}}, \tau_{j+1})$ is a dynamic or slip phase, itself subdivided into dynamic subphases. The trajectory $x(t)$ is completely defined by this cascade of phases and subphases.

2.3.4. Quasistatic approximation when $b(x,t) = K(\beta T(t) - x)$, $T(t)$ slow

Since Eq. (21) is transcendental, we need also an algorithm to solve it. We are going to state an approximation which simplifies considerably the calculations. This approximation is called quasistatic which means that the excitation variation is slow enough to be neglected during any dynamic phase. From then on, an interesting consequence of this approximation is that there are no subphases in the dynamic phases. We will see below that, with the definition of sub phases of Section 2.3.1. in mind, one has x_j^1 and τ_j^1 satisfy

$$|K(\beta T(\tau_j^1) - x_j^1)| \leq f_s.$$

So there is only one sequence τ_j, x_j and once $\tau_{j+\frac{1}{2}}$ is defined, the equation for τ_j^1 becomes simply an equation for τ_{j+1} which is

$$x_j \sin\omega\left(\tau_{j+1} - \tau_j\right) = \int_{\tau_j}^{\tau_{j+1}} \cos\omega(\tau_{j+1} - s) \frac{K\beta T(s) - \epsilon_j f_d}{m\omega} \mathrm{d}s. \tag{23}$$

with

$$\epsilon_j \triangleq \mathrm{sign}(\beta T(\tau_{j+\frac{1}{2}}) - x_j).$$

Next finding x_{j+1} uses Eq. (22) as follows:

$$x_{j+1} \triangleq x_j \cos\omega\left(\tau_{j+1} - \tau_{j+\frac{1}{2}}\right) + \int_{\tau_{j+\frac{1}{2}}}^{\tau_{j+1}} \sin\omega(\tau_{j+1} - s) \times \frac{K\beta T(s) - \epsilon_j f_d}{m\omega} \mathrm{d}s. \tag{24}$$

The quasistatic approximation consists in making the approximation

$$\forall s \in (\tau_{j+\frac{1}{2}}, \tau_{j+1}), \quad T(s) = T(\tau_{j+\frac{1}{2}}).$$

We will use the notation $T_{j+\frac{1}{2}} \triangleq T(\tau_{j+\frac{1}{2}})$. From (24), we obtain

$$\sin(\omega(\tau_{j+1} - \tau_{j+\frac{1}{2}})) = 0$$

which implies

$$\tau_{j+1} = \tau_{j+\frac{1}{2}} + \frac{\pi}{\omega}.$$

We turn to (24) which simplifies considerably using

$$|\beta T_{j+\frac{1}{2}} - x_j| = \frac{f_s}{K}, \tag{25}$$

and we obtain

$$x_{j+1} = x_j + 2\epsilon_j \frac{f_s - f_d}{K}. \tag{26}$$

Of course, we need to find

$$\tau_{j+\frac{1}{2}} = \inf\{t > \tau_j,\ |\beta T(t) - x_j| > \frac{f_s}{K}\}$$

and then define

$$\tau_{j+1} = \tau_{j+\frac{1}{2}} + \frac{\pi}{\omega}.$$

Also

$$\epsilon_{j+1} \triangleq \mathrm{sign}(\beta T_{j+\frac{3}{2}} - x_{j+1}).$$

When we are in a static phase at the value x_j, starting at τ_j, we can interpret the condition (25) as a condition that the future temperature must satisfy to initiate a new dynamic phase.

Remark 5. When $f \triangleq f_s = f_d$, we have seen in Remark 4 that the problem is simply

$$\forall \varphi \in \mathbb{R},\ (K(\beta T(t) - x(t)) - m\ddot{x}(t))(\dot{x}(t) - \varphi) + f|\dot{x}(t)| \leq f|\varphi| \tag{27}$$

with

$$x(0) = x_0,\ \dot{x}(0) = 0.$$

In this case, we also see from the approximation formula (26) that x_j is constant. So the system enters in the static mode at the same point. Since in our assumption $\dot{x}(0) = 0$ and $x(0) = x_0$, we have $x_j = x_0$. This is only an approximation. The alternance of static and dynamic modes follows the sequence of times, $\tau_j, \tau_{j+\frac{1}{2}}$, such that

$$\tau_{j+\frac{1}{2}} = \inf\left\{t > \tau_j \mid T(t) \notin \left[\frac{x_0}{\beta} - \frac{f}{\beta K}, \frac{x_0}{\beta} + \frac{f}{\beta K}\right]\right\} \tag{28}$$

$$\tau_{j+1} - \tau_{j+\frac{1}{2}} = \frac{\pi}{\omega}$$

with $\tau_0 = 0$. What is not an approximation is the following discussion. In a static mode $\tau_j \leq t \leq \tau_{j+\frac{1}{2}}$, we have

$$|\beta T(t) - x(t)| \leq \frac{f}{K} \tag{29}$$

and in a dynamic mode, $\tau_{j+\frac{1}{2}} \leq t \leq \tau_{j+1}$ we have the equation

$$m\ddot{x}(t) = K(\beta T(t) - x(t)) - \epsilon_j f_s \tag{30}$$

and $x(t)$ is C^1, with $\ddot{x}(t)$ locally bounded.

3. Simulations: a step by step Euler method for the discrete version of the two-phase model

Let $T > 0, N \in \mathbb{N}^\star$ and $\{t_n\}_{n=0}^N$ a family of time which discretizes $[0,T]$ such that $t_n \triangleq nh$ where $h \triangleq \frac{T}{N}$. We will construct a sequence $\{(X^h_{t_n}, \dot{X}^h_{t_n})\}_{n=0}^N$ where for each n, $(X^h_{t_n}, \dot{X}^h_{t_n})$ is meant to approximate $(x(t_n), \dot{x}(t_n))$. For each n, from the state $(X^h_{t_n}, \dot{X}^h_{t_n})$ at time t_n, our procedure below defines a unique $(X^h_{t_{n+1}}, \dot{X}^h_{t_{n+1}})$ at the following time t_{n+1}.

3.1. Case $f_d < f_s$

When f_d and f_s are not identical, the dynamics of $x(t)$ is governed by the two-phase model for which the dynamic phase remains governed by $(\mathcal{VI})$ but not the static phase. The finite difference method becomes

$X^h_{t_0} \triangleq x_0,\ \dot{X}^h_{t_0} \triangleq 0$

then for $n = 0, 1, \ldots, N-1$

$X^h_{t_{n+1}} \triangleq X^h_{t_n} + h\dot{X}^h_{t_n}$

and $\dot{X}^h_{t_{n+1}}$ is defined using a discrete version of a two-phase model:

- if
$$\left|\dot{X}^h_{t_n} + \frac{h}{m} b(X^h_{t_n}, t_n)\right| \leq \frac{h}{m} f_s$$
then
$$\dot{X}^h_{t_{n+1}} \triangleq 0.$$
- if
$$\left|\dot{X}^h_{t_n} + \frac{h}{m} b(X^h_{t_n}, t_n)\right| > \frac{h}{m} f_s$$
then $\dot{X}^h_{t_{n+1}}$ is defined as the unique solution of the discrete V.I.
$$\forall \varphi \in \mathbb{R},\ \left(b(X^h_{t_n}, t_n) - m\left(\frac{\dot{X}^h_{t_{n+1}} - \dot{X}^h_{t_n}}{h}\right)\right)(\varphi - \dot{X}^h_{t_{n+1}}) + f_d|\dot{X}^h_{t_{n+1}}| \leq f_d|\varphi|.$$
which means
$$\dot{X}^h_{t_{n+1}} \triangleq \dot{X}^h_{t_n} + \frac{h}{m}\left(b(X^h_{t_n}, t_n) - f_d\epsilon^h_{t_n}\right),$$
$$\epsilon^h_{t_n} \triangleq \operatorname{sign}\left(\dot{X}^h_{t_n} + \frac{h}{m} b(X^h_{t_n}, t_n)\right).$$

3.2. Case $f_d = f_s$

When $f \triangleq f_d = f_s$, the dynamics of $x(t)$ is governed by the variational inequality $(\mathcal{VI})$. Thus a finite difference method leads to a discrete V.I. as follows:

$X^h_{t_0} \triangleq x_0,\ \dot{X}^h_{t_0} \triangleq 0$

then for $n = 0, 1, \ldots, N-1$

$X^h_{t_{n+1}} \triangleq X^h_{t_n} + h\dot{X}^h_{t_n}$

and $\dot{X}^h_{t_{n+1}}$ is defined as the unique solution of the discrete V.I.

$$\forall \varphi \in \mathbb{R},\ \left(b(X^h_{t_n}, t_n) - m\left(\frac{\dot{X}^h_{t_{n+1}} - \dot{X}^h_{t_n}}{h}\right)\right)(\varphi - \dot{X}^h_{t_{n+1}}) + f|\dot{X}^h_{t_{n+1}}| \leq f|\varphi|$$

which is equivalent to defining $\dot{X}^h_{t_{n+1}}$ using a discrete version of a two-phase model in this way:

- if
$$\left|\dot{X}^h_{t_n} + \frac{h}{m} b(X^h_{t_n}, t_n)\right| \leq \frac{h}{m} f$$
then
$$\dot{X}^h_{t_{n+1}} \triangleq 0.$$
- if
$$\left|\dot{X}^h_{t_n} + \frac{h}{m} b(X^h_{t_n}, t_n)\right| > \frac{h}{m} f$$
then
$$\dot{X}^h_{t_{n+1}} \triangleq \dot{X}^h_{t_n} + \frac{h}{m}\left(b(X^h_{t_n}, t_n) - f\epsilon^h_{t_n}\right), \quad \text{where } \epsilon^h_{t_n} \triangleq \operatorname{sign}\left(\dot{X}^h_{t_n} + \frac{h}{m} b(X^h_{t_n}, t_n)\right).$$

Remark 6. When $f \triangleq f_d = f_s$ i.e. when globally the dynamics is governed by a V.I. then the convergence of the solution of the discrete problem toward the solution of the continuous problem is known [16]. Using the notation $u(t) \triangleq (x(t), \dot{x}(t))^T$ and $u_0 \triangleq (x_0, 0)^T$, we can recast Eqs. (1) and (2) in terms of a certain type of differential inclusion as follows:

$$\begin{cases} \dot{u}(t) + \partial\psi(u(t)) \ni g(t, u(t)), & \text{a.e. on } (0,T) \\ u(0) = u_0 \end{cases}$$

where $\forall \mathfrak{u} \triangleq (x,y) \in \mathbb{R}^2$, $\psi(\mathfrak{u}) \triangleq f|y|$ and $g(t,\mathfrak{u}) \triangleq (y, b(x,t))^T$. In particular we recall that

$$\partial\psi(\mathfrak{u}) = \begin{cases} \{\pm f\} \times \{0\} & \text{if } \pm y > 0 \\ [-f, f] \times \{0\} & \text{if } y = 0. \end{cases}$$

For instance, it is clear that if we consider the case of a harmonic forcing $b(x,t) \triangleq K(\beta\cos(\omega t) - x)$ where $K, \beta, \omega > 0$ then

$$\sup_{0\leq t\leq T} \sup_{\mathfrak{u}\neq\mathfrak{v}} \frac{|g(t,\mathfrak{u}) - g(t,\mathfrak{v})|_{\mathbb{R}^2}}{|\mathfrak{u} - \mathfrak{v}|_{\mathbb{R}^2}} < \infty$$

and also $\frac{\partial g}{\partial t}(t,\mathfrak{u})$ is bounded on $[0,T]$ and does not depend on $\mathfrak{u}$. Here $|.|_{\mathbb{R}^2}$ is a norm on $\mathbb{R}^2$. In this context, Theorem 3.1 of [16] can be applied. There exists a constant $M \geq 0$ such that

$$\forall h > 0,\ \|u - u^h\| \triangleq \sup_{0\leq t\leq T} |u(t) - u^h(t)|_{\mathbb{R}^2} \leq Mh.$$

where $u^h(.)$ is the linear interpolation of $(X^h_{t_n}, \dot{X}^h_{t_n})$ on $[0,T]$. The order of the method is one.

3.3. Two numerical case studies

In this section, we apply the algorithm presented in Section 3.1 to two cases. The first one concerns the response of a system with dry friction to harmonic excitation. The second one is similar to the first one except that it includes an additional random perturbation expressed as an Ornstein–Uhlenbeck process. To support the validity of the numerical method, we also discuss the empirical rate of convergence of the algorithm in these two cases.

3.3.1. Simulation of the response of a system with dry friction to harmonic excitation

We consider the model studied by Shaw in [2]. We apply the algorithm above to simulate $x(t)$ satisfying (1) where the right hand side is of the form

$$b(x(t), t) \triangleq \beta\cos(\omega t) - x(t). \tag{31}$$

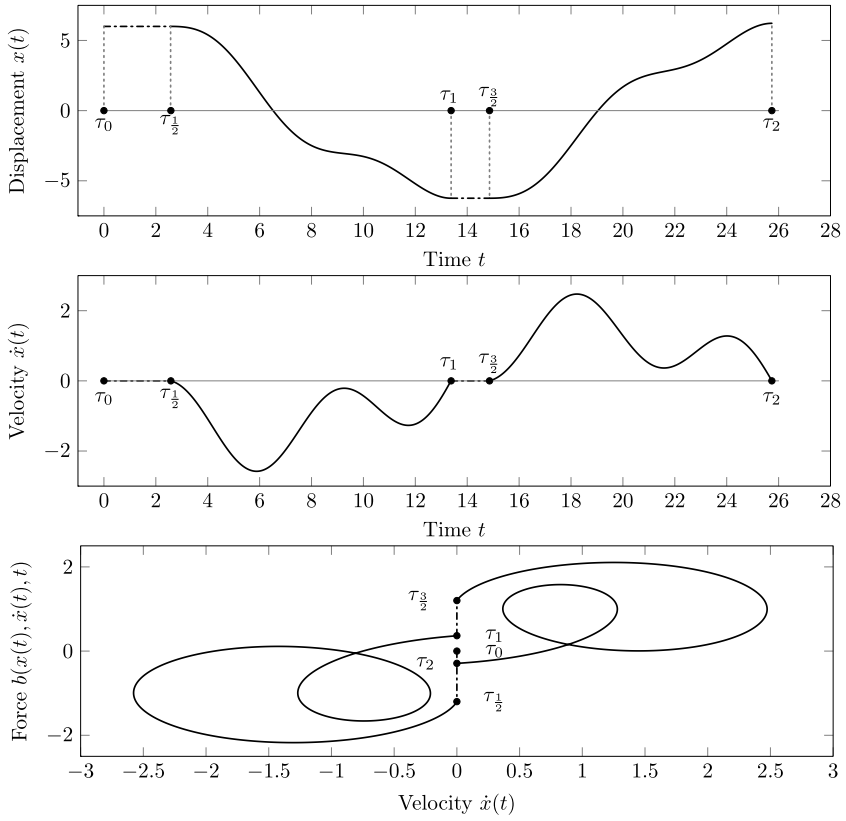

Fig. 1. Simulation of trajectories. Typical trajectory of a solution $x(t)$ with an harmonic forcing (Eq. (1) with (31)). The numerical results have been obtained using the numerical scheme shown in Section 3. The time intervals enclosed by $[\tau_0, \tau_{\frac{1}{2}})$ and $[\tau_1, \tau_{\frac{3}{2}})$ correspond to static phases whereas the intervals $[\tau_{\frac{1}{2}}, \tau_1)$ and $[\tau_{\frac{3}{2}}, \tau_2)$ correspond to dynamic phases.

To ensure sticking motions, we chose the parameters as follows

$$m = 1,\ f_d = 1,\ f_s = 1.2,\ \beta = 6,\ \omega = \frac{1}{2}. \qquad (\mathcal{P})$$

This choice is inspired from Figure 8 p. 315 in [2]. The numerical results are shown in Fig. 1. We recover the results obtained by [2].

3.3.2. Simulation of the response of a system with dry friction to a random perturbation

Using the numerical scheme above, the behavior of (1)–(2) has been simulated with a temperature function chosen as $T(t) = \cos(\omega t) + \rho v(t)$ where $v(t)$ is an Ornstein–Uhlenbeck noise in the sense that

$$\dot{v} = -v + \dot{w}, \quad \text{where } w \text{ is a Wiener process.}$$

This can be seen as a random perturbation of the model on the section above. Here ρ is a small parameter. Fig. 2 displays the result of the simulation. We used the parameters $(\mathcal{P})$ and $K = 1$, $\rho = 0.25$. Fig. 2 displays the displacement $x(t)$ in response to $\beta T(t)$, and the velocity $\dot{x}(t)$ together with the forces $\mathbb{F}(\dot{x}(t))$ and $K(\beta T(t) - x(t))$. Fig. 2**C** displays the evolution of $(\beta T(t) - x(t), \dot{x}(t))$ with respect to t in a displacement versus temperature plane. The static phases occur during the time intervals $(\tau_j, \tau_{j+\frac{1}{2}})$. They can be seen in Fig. 2 when $x(t)$ is constant (Fig. 2**A**) or $\dot{x}(t) = 0$ (Fig. 2**B**) over time intervals with positive Lebesgue measure. In contrast, the dynamic phases occur during the time intervals $(\tau_{j+\frac{1}{2}}, \tau_{j+1})$. They can be seen in Fig. 2**B** as non constant phases and in Fig. 2**C** as cycles. In this simulation, there are subphases in the dynamic phases. The likeliness of occurrence of dynamic sub phases is highly dependent on important variations of the temperature $T(t)$.

3.3.3. Empirical accuracy in the numerical case study

Below, we use the same notation as in Remark 6. For instance, the notation u is for $(x, \dot{x})$ and u^h is for the linear interpolation of $(X^h_{t_n}, \dot{X}^h_{t_n})$ on $[0, T]$. If the numerical method is of order p with p is a certain positive number then $\|u^h - u\| \leq Ch^p$ where C is a constant independent of h. Moreover, if in addition $\|u^h - u\| = Ch^p + O(h^{p+\epsilon})$ for some $\epsilon > 0$ then

$$\frac{\|u^h - u^{\frac{h}{2}}\|}{\|u^{\frac{h}{2}} - u^{\frac{h}{4}}\|} \approx 2^p + O(h^\epsilon).$$

With such a relation in mind, we empirically test the convergence of our algorithm by considering ratios involving the norm of the difference between u^h computed for different h halved successively. To be precise, we look at the behavior of

$$q(h) \triangleq \frac{\|u^h - u^{\frac{h}{2}}\|}{\|u^{\frac{h}{2}} - u^{\frac{h}{4}}\|}$$

and $p(h) \triangleq \log_2(q(h))$. With $T = 5$ and other parameters unchanged, $h_0 = 0.05$ and for different values of $h \in \{h_0 2^{-j},\ 0 \leq j \leq 7\}$, in Table 1 we present a set of empirical estimations of $p(h)$ in the two numerical case studies. The data indicates that the convergence rate of the method is $\sim h$, i.e the numerical method is empirically of order 1.

4. Experimental campaign

In general, mechanical properties of real world structures are not known but in some cases it is possible to infer them from observations (experimental data). Here, we focus on the behavior of such a structure (bridge component) subjected to changes of

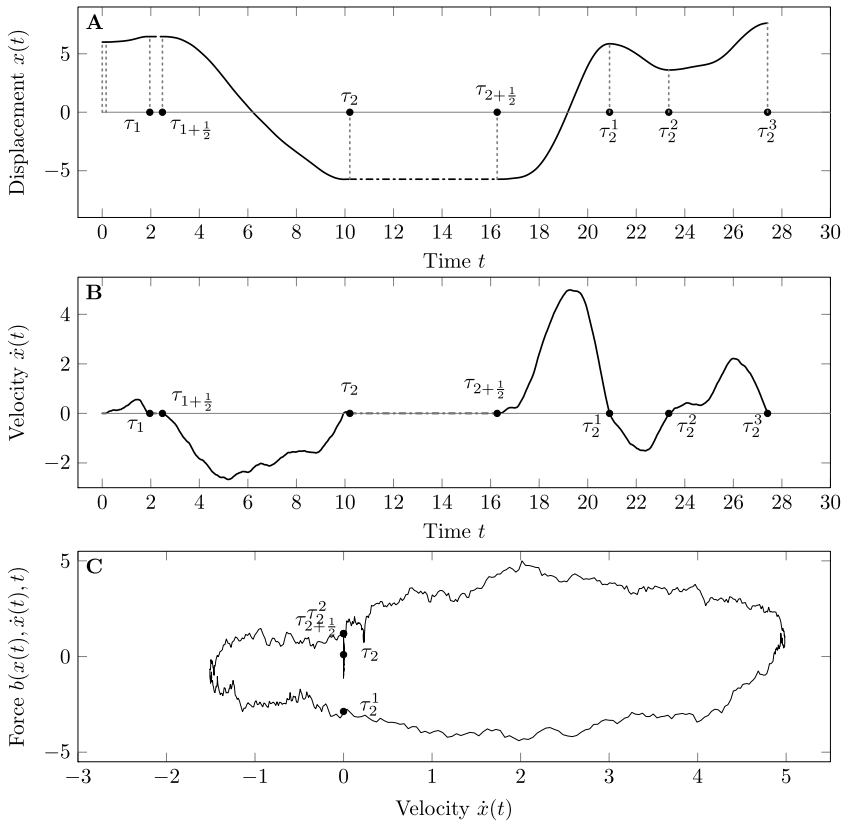

Fig. 2. Simulation of trajectories. Typical trajectory of a solution $x(t)$ where the temperature function T is given by $T(t) = \cos(\omega t) + \rho v(t)$ where v is an Ornstein–Uhlenbeck process, $\rho = 0.25$. The $\tau_\bullet$ and $\tau_\bullet^\bullet$ pinned on the trajectory refer to the times defined in Section 2.3.

Table 1
Empirical rate of convergence with different h, starting with $h_0 \triangleq 0.05$ halved successively: (a) case of harmonic excitation and (b) case of harmonic excitation perturbed by an Ornstein–Uhlenbeck process.

(a)			(b)		
h	$\|u^h - u^{\frac{h}{2}}\|$	$p(h)$	h	$\|u^h - u^{\frac{h}{2}}\|$	$p(h)$
h_0	0.26284	1.01745	h_0	0.41406	1.12726
$h_0 2^{-1}$	0.12984	1.04446	$h_0 2^{-1}$	0.18955	0.99567
$h_0 2^{-2}$	0.06295	1.01035	$h_0 2^{-2}$	0.09506	0.94579
$h_0 2^{-3}$	0.03125	1.00509	$h_0 2^{-3}$	0.04935	1.10016
$h_0 2^{-4}$	0.01557	1.00278	$h_0 2^{-4}$	0.02302	0.96288
$h_0 2^{-5}$	0.00777	0.97606	$h_0 2^{-5}$	0.01181	1.07137
$h_0 2^{-6}$	0.00395	1.02580	$h_0 2^{-6}$	0.00562	1.16864

temperatures over time, see Fig. 3. Engineers are interested in inferring the initial condition of displacement and other properties of the structure such as the stiffness, the magnitude of the static and dynamic friction forces and the dilatation with respect to the temperature. In terms of our model, it corresponds to adjusting the parameters z_0, K, f_s, f_d and β to fit a set of observations.

4.1. Presentation of the experimental data

The model described above has been used on a practical case study on the Paris Metro Line 6 in 2016. The aim of the operation was to estimate the real friction coefficients f_s and f_d of a single bearing point of the metro viaduct, near to the station Quai de la Gare in the East of Paris. The viaduct is an isostatic steel truss built in 1909. The bearing points are supposed to be fixed at one end and free at the other end of each span, but actually a significant friction appears on the free bearing points. OSMOS Group performed the continuous monitoring of the displacement of the span end on one of the free bearing points during one full year in 2015 and 2016. The measurements were taken 6 times every hour and additional records with 50 points every second were also available under the effects of the live loads. The bridge is instrumented with multiple sensors which measure (a) T_{xp} the temperature in Celsius degree and (b) z_{xp} the displacement sensor in millimeters. The period of data assimilation covers about ∼300 days (August 2015–May 2016). See Fig. 4. It is important to emphasize that the output of the displacement sensor $z_{\text{xp}}(t)$ is actually the sum of the bearing point displacement and the elastic shear deformation, as shown in Fig. 3. The bearing point has a linear behavior, and its stiffness is known $K_{\text{BP}} = 2.0 \times 10^6\,\text{N m}^{-1}$. For the sake of consistency with the experimental data, in our numerical results we also use a corrected variable $z(t)$ that takes the elastic shear deformation into account $z(t) = x(t) + F(t)/K_{\text{BP}}$.

4.2. Calibration of the model to interpret the experimental data

The experimental data, discussed in the previous section, showed that the length of a dynamic phase is smaller than the acquisition time-step. Moreover, since this time-step is sufficiently small, the temperature variation between two time steps is also relatively small. Therefore, we consider that the changes of temperature during dynamic phases are not significant. Physically, that justifies the use of the quasi-static approximation in the model for interpreting the data. Now, the goal is to find a set of parameters for the model that gives a good fit between the numerical and the experimental results. The parameters considered are: a constant displacement offset z_0, the stiffness K, the dilatation coefficient β and the two friction coefficients f_s and f_d. It is a difficult task to calibrate the model but one can use a least-square method and minimize the function:

$$\text{err}(z_0, K, \beta, f, f_0) = \int \left(z_0 + z^{K,\beta,f,f_0}(T_{\text{xp}}(s)) - z_{\text{xp}}(s)\right)^2 ds \qquad (32)$$

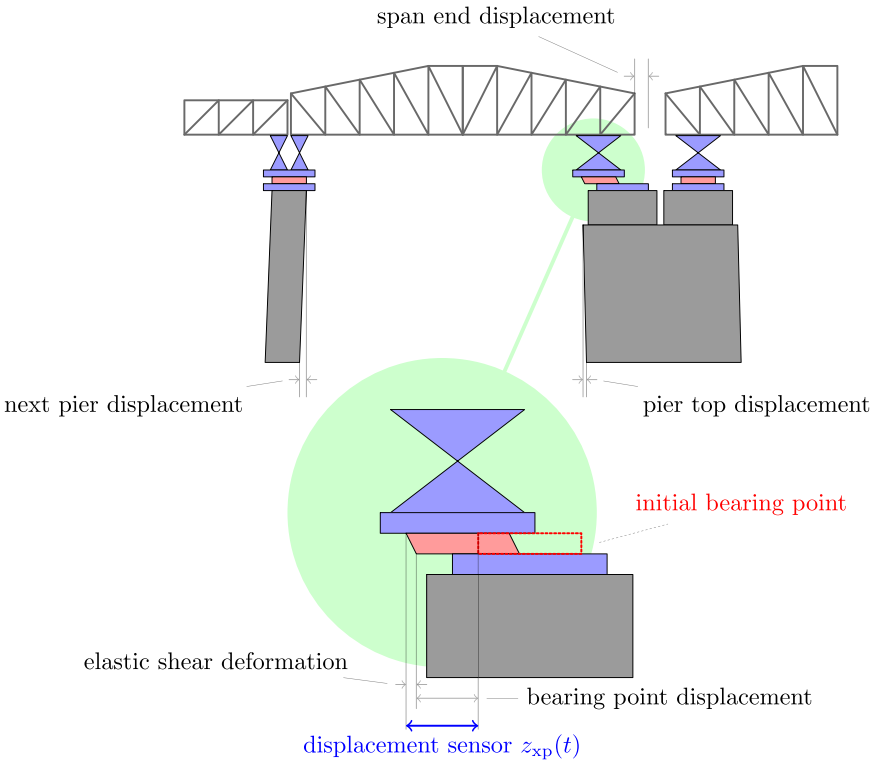

Fig. 3. The structure consists of a pier (massive solid block) that is located between a bridge (horizontal structure) and its base. The pier is driven by a thermally induced displacement forcing and experiences dry friction (due to bridge/pier interaction). This mechanical structure is located at the Parisian metro station Quai de la Gare (courtesy of RATP, the main public transportation in Paris).

Table 2
Results for 10 optimization procedures with different random initial sets of values.

Run #	z_0 [m]	K [N m^{-1}]	f_d [N]	f_s [N]	β [m K^{-1}]
1	$9.54 \cdot 10^{-3}$	$1.75 \cdot 10^{5}$	0.42	0.47	$2.97 \cdot 10^{-4}$
2	$9.18 \cdot 10^{-3}$	$2.06 \cdot 10^{8}$	0.42	0.47	$2.72 \cdot 10^{-4}$
3	$9.84 \cdot 10^{-3}$	$1.81 \cdot 10^{8}$	0.42	0.47	$3.18 \cdot 10^{-4}$
4	$9.78 \cdot 10^{-3}$	$1.93 \cdot 10^{8}$	0.43	0.49	$3.14 \cdot 10^{-4}$
5	$9.77 \cdot 10^{-3}$	$1.98 \cdot 10^{8}$	0.44	0.47	$3.14 \cdot 10^{-4}$
6	$9.78 \cdot 10^{-3}$	$1.85 \cdot 10^{8}$	0.42	0.47	$3.13 \cdot 10^{-4}$
7	$9.74 \cdot 10^{-3}$	$1.8 \cdot 10^{8}$	0.4	0.45	$3.12 \cdot 10^{-4}$
8	$9.72 \cdot 10^{-3}$	$1.83 \cdot 10^{8}$	0.42	0.46	$3.1 \cdot 10^{-4}$
9	$9.71 \cdot 10^{-3}$	$1.9 \cdot 10^{8}$	0.43	0.48	$3.08 \cdot 10^{-4}$
10	$9.67 \cdot 10^{-3}$	$1.97 \cdot 10^{8}$	0.43	0.45	$3.06 \cdot 10^{-4}$
Mean	$9.67 \cdot 10^{-3}$	$1.89 \cdot 10^{8}$	0.42	0.47	$3.06 \cdot 10^{-4}$
St. D.	$1.91 \cdot 10^{-4}$	$9.67 \cdot 10^{6}$	$1.12 \cdot 10^{-2}$	$1.17 \cdot 10^{-2}$	$1.34 \cdot 10^{-5}$
C. V.	$1.97 \cdot 10^{-2}$	$5.12 \cdot 10^{-2}$	$2.65 \cdot 10^{-2}$	$2.5 \cdot 10^{-2}$	$4.38 \cdot 10^{-2}$

where the time integration is done over the data assimilation period ($\sim$300 days), $T_{xp}(s)$ and $z_{xp}(s)$ are the experimental data for the temperature and the displacement respectively, and $z^{K,\beta,f,f_0}(T_{xp}(s))$ is the displacement given by the model detailed in Section 2.3 with the quasistatic approximation, with K, β, f_d, f_s as parameters and with $T_{xp}(s)$ as temperature input. We use the genetic algorithm of the MATLAB optimization toolbox [17] to look for the minimum of the function err. We have performed 10 tests with different arbitrary initial sets of parameters, we obtain the values presented in Table 2.

4.3. Comparison between the experimental observations and our calibrated model

Using the parameters shown in the first row of Table 2, we have obtained numerical results of our calibrated model in response to the observed thermal forcing. These results are compared to the experimental observations in Figs. 4 and 5. Fig. 4 presents the results over time; the main plot displays them over a 9 months period and the two other plots display a zoomed in result over a 2 month period. Each of those plots displays on the top part both the measured and computed displacements, and on the bottom part the measured temperature. Fig. 5 displays both the experimental and numerical results in the *displacement versus temperature* phase plan. The loops predicted by the model have a similar width and height than those obtained with the experimental data. Good agreement between experimental and numerical data is shown on these figures. That supports that the model is quite accurate. This practical case study enables to validate the friction model and to identify the friction coefficients of the bearing point.

5. Conclusion

An extended variational inequality (EVI) approach is introduced for modeling dry friction when essentially the forcing is

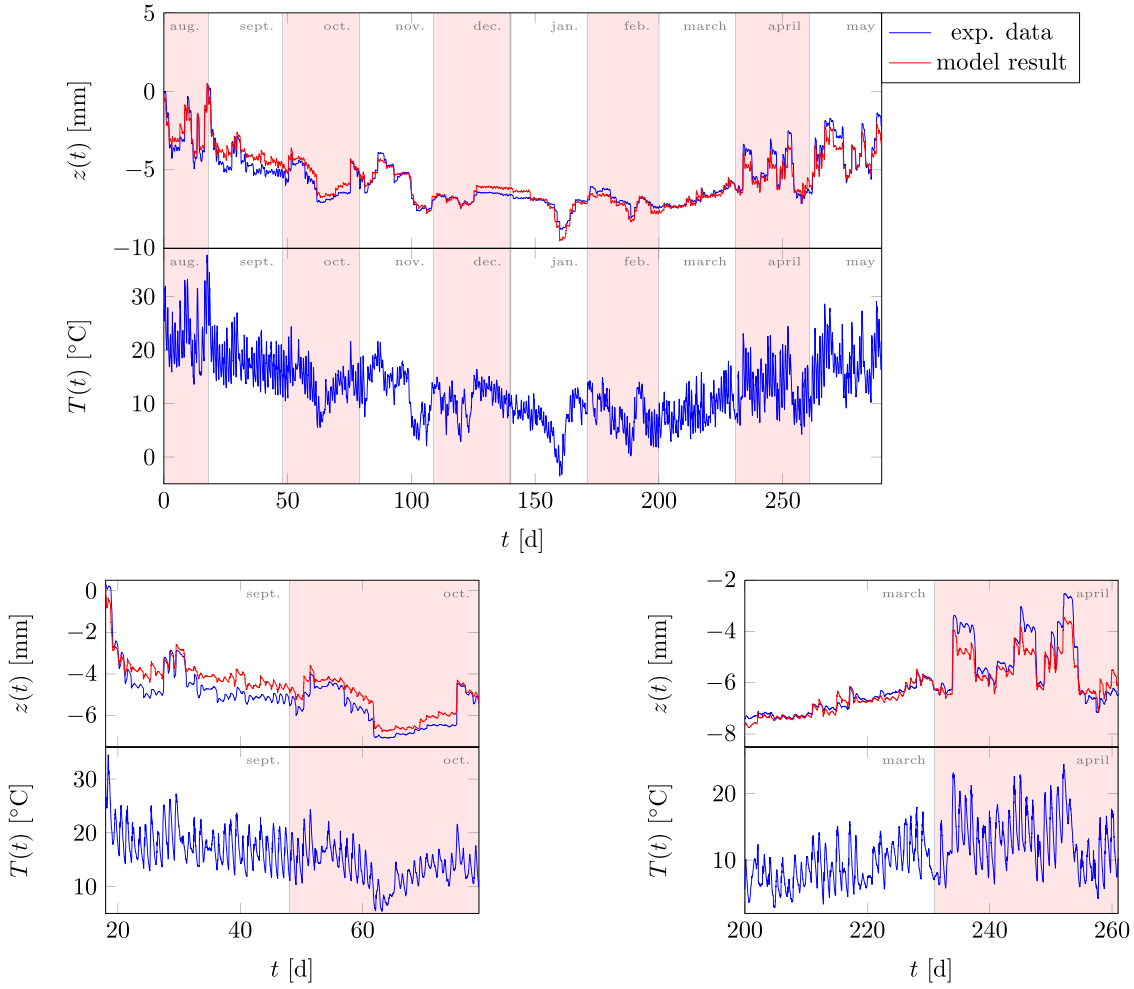

Fig. 4. Experimental and numerical results according to time. Main : 1 data point per hour. Zooms : 1 data point per 10 min.

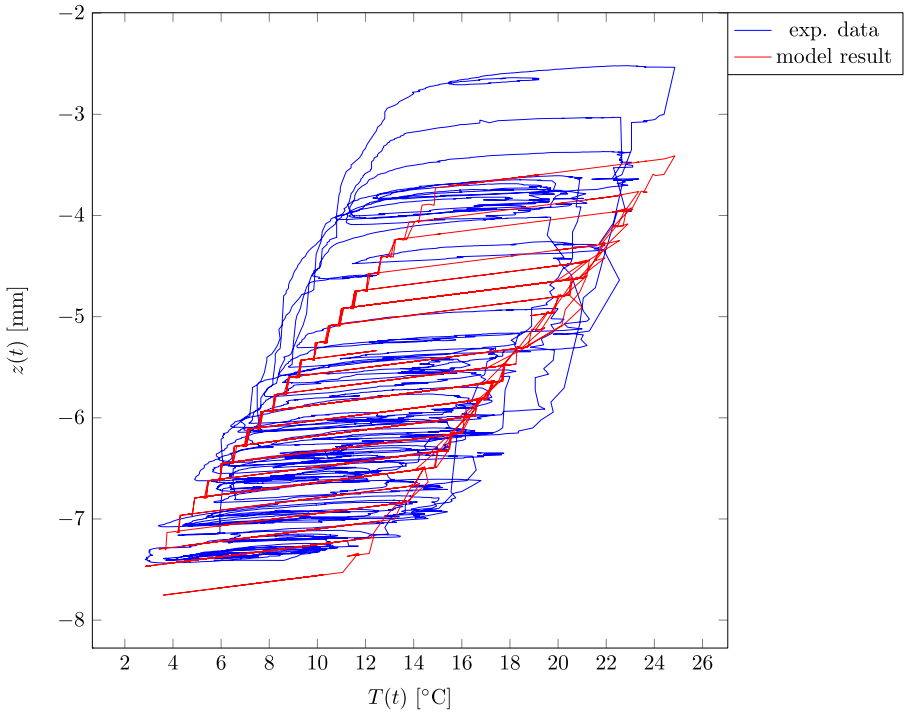

Fig. 5. Experimental and numerical results in the *displacement versus temperature plane*. For the convenience of the reader, we only display the data for March and April. 1 data point per 10 min.

assumed to be a continuous time function. A proof of existence and uniqueness is given when f_s the coefficient of static friction is larger than f_d the coefficient of dynamic friction. When f_s and f_d are identical, our approach turns out to be equivalent to a standard variational inequality [18]. Then, for simulation purpose, a discrete time version of the EVI approach is proposed in terms of a step by step Euler method. This discrete problem is well posed. In practice, the method is simple to implement with any programming language such as MATLAB or C. When f_s and f_d are identical, the rate of convergence of the solution to the discrete time problem toward the solution of the continuous time problem is known [16]. The method is of order one. In contrast, when f_s and f_d are different, the study of the rate of convergence remains an open question which is beyond the scope of this work. However, numerical test studies indicate an empirical rate of convergence of order one. Next, our framework is used on a practical case study where the objective is to estimate the friction coefficients f_s and f_d associated to a real world structure. The latter is a single bearing point of the metro viaduct, near to the station Quai de la Gare in the East of Paris. The viaduct is an isostatic steel truss built in 1909. The bearing points are supposed to be fixed at one end and free at the other end of each span, but actually a significant friction appears on the free bearing points. Here the forcing $b(x, t)$ is of the form $K(\beta T(t) - x)$ where T has slow variation. In this context, a quasi static approximation of the EVI is used to interpret the data. There are 5 parameters for an acquisition period of the experimental data of $\sim$300 days with a measurement every 10 min. OSMOS Group performed the continuous monitoring of the displacement of the span end on one of the free bearing points during one full year in 2015 and 2016. Our model fitted with these parameters matches the available data closely. We have used a standard algorithm encoded in MATLAB to minimize the error function. In this context a minimizer has been obtained. Perhaps more sophisticated algorithms can possibly do better. This type of issues (including the convexity of the error function) is beyond the scope of the present paper. Finally, we would like to emphasize that an important benefit of our EVI approach together with its discrete time counterpart is that it can be employed for a broad class of functions $b(x, y, t)$. We recall that the latter represent forces that are not related to dry friction. Moreover, there is strictly no conceptual difficulty to adapt our method to any multi degree of freedom (MDOF) system involving several nonlinear behaviors such as dry friction, while keeping a synthetic framework.

Declaration of competing interest

The authors declare that they have no known competing financial interests or personal relationships that could have appeared to influence the work reported in this paper.

Acknowledgments

Alain Bensoussan's research is supported by the National Science Foundation, USA under the grant DMS-1905449, the grant from the SAR Hong Kong RGC GRF 11303316 and EREN groupe. Laurent Mertz is supported by the National Natural Science Foundation of China, Young Scientist Program #11601335. The authors wish to thank RATP Infrastructures for its support in the publication of the results on the Paris Metro Line 6 case. Alain Bensoussan and Laurent Mertz wish to thank Jérôme Bastien for an extremely interesting exchange about differential inclusions which allowed to clarify their present approach in terms of an extended variational inequality.

References

[1] J.P. Den Hartog, Forced vibrations with combined Coulomb and viscous damping, Trans. Am. Soc. Mech. Eng. 53 (1930) 107–115.
[2] S.W. Shaw, On the dynamic response of a system with dry friction, J. Sound Vib. 108 (2) (1986) 305–325.
[3] C. Pierre, A. Ferri, E. Dowell, Multi–harmonic analysis of dry friction damped systems using an incremental harmonic balance method, Trans. Am. Soc. Mech. Eng. 52 (4) (1985) 958–964.
[4] G.C.K. Yeh, Forced vibrations of a two-degree-of-freedom system with combined Coulomb and viscous damping, J. Acoust. Soc. Am. 39 (1966) 14.
[5] S.L. Lau, Y.K. Cheung, S.Y. Wu, A variable parameter incremental method for dynamic instability of linear and nonlinear elastic systems, ASME J. Appl. Mech. 49 (1982) 849–853.
[6] S.L. Lau, Y.K. Cheung, S.Y. Wu, Incremental harmonic balance method with multiple time scales for aperiodic vibration of nonlinear systems, ASME J. Appl. Mech. 50 (1983) 871–876.
[7] V.L. Popov, Contact Mechanics and Friction. Physical Principles and Applications, Springer Berlin Heidelberg, 2010.
[8] https://ocw.mit.edu/courses/physics/8-01sc-classical-mechanics-fall-2016/week-2-newtons-laws/dd.1.1-friction-at-the-nanoscale/.
[9] H. Brézis, Opérateurs Maximaux Monotones et Semi-Groupes de Contractions Dans Les Espaces de Hilbert. (French) North-Holland Mathematics Studies, in: Notas de Matemática (50), (5) North-Holland Publishing Co. Amsterdam-London; American Elsevier Publishing Co. Inc., New York, 1973, p. vi+183.
[10] Frédéric Lebon, Contact problems with friction: Models and simulations, in: Simulation Modelling Practice and Theory, Vol. 11, Elsevier, 2003, pp. 449–464.
[11] Manuel D.P. Monteiro Marques, Differential Inclusions in Nonsmooth Mechanical Problems. Shocks and Dry Friction. Progress in Nonlinear Differential Equations and their Applications, Vol. 9, Birkhäuser Verlag, Basel, ISBN: 3-7643-2900-9, 1993, p. x+179.
[12] J. Bastien, M. Schatzman, Indeterminacy of a dry friction problem with viscous damping involving stiction, ZAMM Z. Angew. Math. Mech. 88 (4) (2008) 243–255.
[13] M. di Bernardo, C.J. Budd, A.R. Champneys, P. Kowalczyk, Piecewise-Smooth Dynamical Systems. Theory and Applications. Applied Mathematical Sciences, Vol. 163, Springer-Verlag London, Ltd., London, ISBN: 978-1-84628-039-9, 2008, p. xxii+481.
[14] G. Licskó, G. Csernák, On the chaotic behaviour of a simple dry-friction oscillator, Math. Comput. Simulation 95 (2014) 55–62.
[15] A. Klarbring, M. Ciavarella, J.R. Barber, Shakedown in elastic contact problems with Coulomb friction, Int. J. Solids Struct. 44 (2007) 8355–8365.
[16] J. Bastien, Convergence order of implicit Euler numerical scheme for maximal monotone differential inclusions, Z. Angew. Math. Phys. 64 (4) (2013) 955–966.
[17] MATLAB Optimization Toolbox, The MathWorks, Natick, MA, USA.
[18] J. Bastien, M. Schatzman, C. Lamarque, Study of some rheological models with a finite number of degrees of freedom, Eur. J. Mech./A Solids 19 (2) (2000) 277–307.